NANO · MICRO small
www.small-journal.com

Smartphone-Flashlight-Mediated Remote Control of Rapid Insulin Secretion Restores Glucose Homeostasis in Experimental Type-1 Diabetes

*Maysam Mansouri, Shuai Xue, Marie-Didiée Hussherr, Tobias Strittmatter, Gieri Camenisch, and Martin Fussenegger**

Emerging digital assessment of biomarkers by linking health-related data obtained from wearable electronic devices and embedded health and fitness sensors in smartphones is opening up the possibility of creating a continuous remote-monitoring platform for disease management. It is considered that the built-in flashlight of smartphones may be utilized to remotely program genetically engineered designer cells for on-demand delivery of protein-based therapeutics. Here, the authors present smartphone-induced insulin release in β-cell line (iβ-cell) technology for traceless light-triggered rapid insulin secretion, employing the light-activatable receptor melanopsin to induce calcium influx and membrane depolarization upon illumination. This iβ-cell-based system enables repeated, reversible secretion of insulin within 15 min in response to light stimulation, with a high induction fold both in vitro and in vivo. It is shown that programmable percutaneous remote control of implanted microencapsulated iβ-cells with a smartphone's flashlight rapidly reverses hyperglycemia in a mouse model of type-1 diabetes.

1. Introduction

Synthetic biology-inspired cell-based therapy relies on engineered mammalian cells that sense a user-defined input signal, process it, and respond appropriately through a customizable therapeutic output.[1,2] Many genetic circuits have been developed that enable engineered cells to produce controlled dosages of therapeutic agents on-demand in response to disease-related biomarkers,[3–7] chemical compounds,[8–10] or physical inducers.[7,11–14] However, most of these circuits are based on genetic switches that induce transcription of a desired therapeutic transgene from a synthetic expression unit upon activation.[15] This transcription-based strategy involves a delay of 6–8 h after induction until the therapeutic protein is produced. This delay is not an issue in the treatment of diseases requiring therapeutics for long-term homeostasis, but in the case of diseases such as type-1 diabetes (T1D), rapid delivery of the therapeutic protein is crucial.[16]

In T1D mellitus, a chronic autoimmune disease, secretion of insulin is impaired due to loss of pancreatic β-cells.[17] This leads to an increase in blood glucose level (hyperglycemia) which, if sustained for over a long period, can cause a range of complications, including renal, vascular, neuronal, and cardiovascular diseases, as well as retinal degeneration and increased cancer risk.[18] In addition, life-threatening emergency situations can arise if the blood glucose level rises too quickly.[19,20] Hence, insulin therapy based on disciplined administration or automated supply of exogenous insulin has been widely utilized for T1D treatment.[21–23] However, manual insulin injection regimes often fail to maintain the protein concentration within the therapeutic window or fail to provide appropriate delivery kinetics.[24]

"Mobile health" is a nascent concept that aims to facilitate patient-physician contact by providing a continuous and remote monitoring communication platform for disease management.[25,26] For this purpose, health-related data are provided through embedded smartphone sensors, for example, for fingertip-mediated evaluation of heart-rate variability (HRV),[27,28] or through other wearable,[29] ingestible,[30] and implantable[31] sensors that can be wirelessly connected to a smartphone. The data flow can aid disease self-management or can be transferred to healthcare professionals for further analysis via the internet of things (IOT).[26,32,33] In addition to the use of smartphones to receive data from wearable electronic biosensors, we considered that it might be feasible to use them to remotely program engineered cells to trigger a rapid, on-demand therapeutic effect. To take this idea forward, we have developed optogenetically engineered designer cells that release

Dr. M. Mansouri, Dr. S. Xue, M.-D. Hussherr, T. Strittmatter, Dr. G. Camenisch, Prof. M. Fussenegger
Department of Biosystems Science and Engineering
ETH Zurich
Mattenstrasse 26, Basel CH-4058, Switzerland
E-mail: fussenegger@bsse.ethz.ch
Prof. M. Fussenegger
Faculty of Science
University of Basel
Mattenstrasse 26, Basel CH-4058, Switzerland

The ORCID identification number(s) for the author(s) of this article can be found under https://doi.org/10.1002/smll.202101939.

DOI: 10.1002/smll.202101939

pre-formed insulin-containing granular vesicles in response to melanopsin-triggered membrane depolarization induced by the flashlight of a smartphone. We confirmed that these iβ-cell lines (smartphone-induced insulin release in β-cells) provide a robust, repeatable, and reversible platform for rapid insulin secretion (within 15 min) upon light stimulation in vitro and in vivo. We show that subcutaneously implanted, microencapsulated, smartphone-controlled engineered human cells can effectively reverse hyperglycemia in type-1 diabetic mice under the control of a smartphone's flashlight.

2. Results

2.1. Design and Validation of iβ-cells

Intracellular levels of second messengers serve to regulate insulin exocytosis in β cells.[34,35] Therefore, to design iβ-cells we focused on well-known light-inducible receptors that trigger endogenous calcium or cAMP pathways upon activation. We co-transfected different light-triggered Gq- or Gs-linked G-protein coupled receptors (GPCRs), including melanopsin, Opto-α1AR and Opto-β2AR,[36] with different synthetic expression units containing responsive elements for calcium, cAMP, and mitogen-activated protein kinase (MAPK) pathways and driving expression of the human placental secreted alkaline phosphatase (SEAP) gene in human embryonic kidney 293 T cells (HEK293T). Cells transfected with melanopsin produced the highest level of SEAP glycoprotein in response to light compared to the other receptors (Figure S1, Supporting Information). We further showed that melanopsin can trigger a calcium response that induces the expression of SEAP from a synthetic reporter construct as efficient as chemically activated GPCR or ion channels (Figure S2, Supporting Information).

To develop a light-controllable therapeutic designer cell with fast kinetics, we used an INS_{vesc} cell line, a variant of the established pancreatic β-cell line 1.1E7.[37] This variant is recalcitrant to glucose levels and also stably expresses a proinsulin-NanoLuc construct encoding an insulin derivative having its C-peptide replaced by *Oplophorus gracilirostris* luciferase (NanoLuc, nLuc).[11,38] INS_{vesc} cells exhibited rapid kinetics of insulin and nLuc secretion upon membrane depolarization induced by potassium chloride (KCl), regardless of the glucose concentration in the medium (Figure S3, Supporting Information). This allows on-demand control of insulin secretion by the user, without interference from blood-glucose level. We also demonstrated that membrane depolarization and insulin-nLuc release in INS_{vesc} cells can occur after activation of ectopically expressed calcium-triggering Gq-linked GPCRs (Figure S4a, Supporting Information). Therefore, melanopsin was stably expressed in INS_{vesc} cells and a monoclonal population termed "iβ-cell" line was generated (Figure S4b–e, Supporting Information). **Figure 1**a shows a schematic representation of light-triggered rapid insulin-nLuc secretion in an iβ-cell. We confirmed that iβ-cells release granules containing insulin and nLuc in a well-correlated ratio within 15 min upon light stimulation (Figure 1b,c).

To establish the role of melanopsin in triggering rapid insulin secretion in iβ-cells, we exposed iβ-cells and parental INS_{vesc} cells to light and confirmed that only iβ-cells expressing melanopsin, and not INS_{vesc} cells, could release insulin-nLuc granules upon illumination (Figure 1d). The functionality of melanopsin for initiating insulin-nLuc release is crucial because iβ-cells grown in media without chromophore (all-*trans* retinal, ATR) were not able to induce insulin-nLuc secretion even if stimulated with blue light (Figure 1e). Furthermore, we showed that iβ-cells respond to blue light emitted from LEDs (Figure 1f) or to bioluminescence (Figure 1g). Activated melanopsin increased the intracellular calcium level in iβ-cells, while inhibitors of calcium signaling blocked insulin-nLuc secretion (Figure S5, Supporting Information).

2.2. Characterization of iβ-Cells

We first measured insulin release dynamics in iβ-cells upon stimulation with light and found that insulin and nLuc activities in the supernatant peaked within 15 min (**Figure 2**a and Figure S6a, Supporting Information). iβ-cells were also tested for reversibility by stimulating them repeatedly with blue light for 15 min followed by a 4 h recovery period in darkness; they displayed excellent reversibility of insulin-nLuc secretion (Figure 2b). Also, iβ-cells maintained a constant basal level of insulin-nLuc release in the presence of various concentrations of glucose, and induction was exclusively triggered by light (Figure 2c). Furthermore, iβ-cells can be stimulated by different light intensities (Figure 2d) and cultured in various systems (adherent or suspension) at various cell densities, while retaining high viability (Figure S6, Supporting Information). Illumination of iβ-cells for only 2 min was sufficient to induce a significant rise of insulin-nLuc level (Figure S6, Supporting Information). We also compared iβ-cells with a melanopsin-mediated transcription-based system expressing insulin-nLuc upon illumination with blue light. Although 15 min of blue light exposure was sufficient to induce insulin-nLuc secretion from iβ-cells, a comparable release level was only achieved after 6 h of illumination in the transcription-based system (Figure 2e). To simulate a real-world application, we illuminated iβ-cells with white light emitted by a commercially available smartphone. This resulted in rapid release of insulin-nLuc granules within 15 min, with comparable efficiency to that of blue light (Figures 2f–h and Figure S7, Supporting Information).

2.3. iβ-Cell-Operated by Smartphone's Flashlight can Mediate Normoglycemia in Experimental Type-1 Diabetes

To study the kinetics of our fast insulin-nLuc release system in vivo, we subcutaneously implanted microencapsulated iβ-cells on the back of mice and exposed them to either a smartphone's white light (**Figure 3**a and Figure S8a, Supporting Information) or ambient light, and compared them to the non-illuminated control group. The white light exposure produced a robust induction profile for insulin-nLuc secretion in the blood of mice, peaking at 30 min, while the group exposed to ambient light showed no induction (Figure 3b and Figure S8b, Supporting Information). In animals exposed to successive light induction cycles for 7 days, the iβ-cells rapidly, reversibly, and repeatedly released insulin-nLuc in response to light (Figure 3c

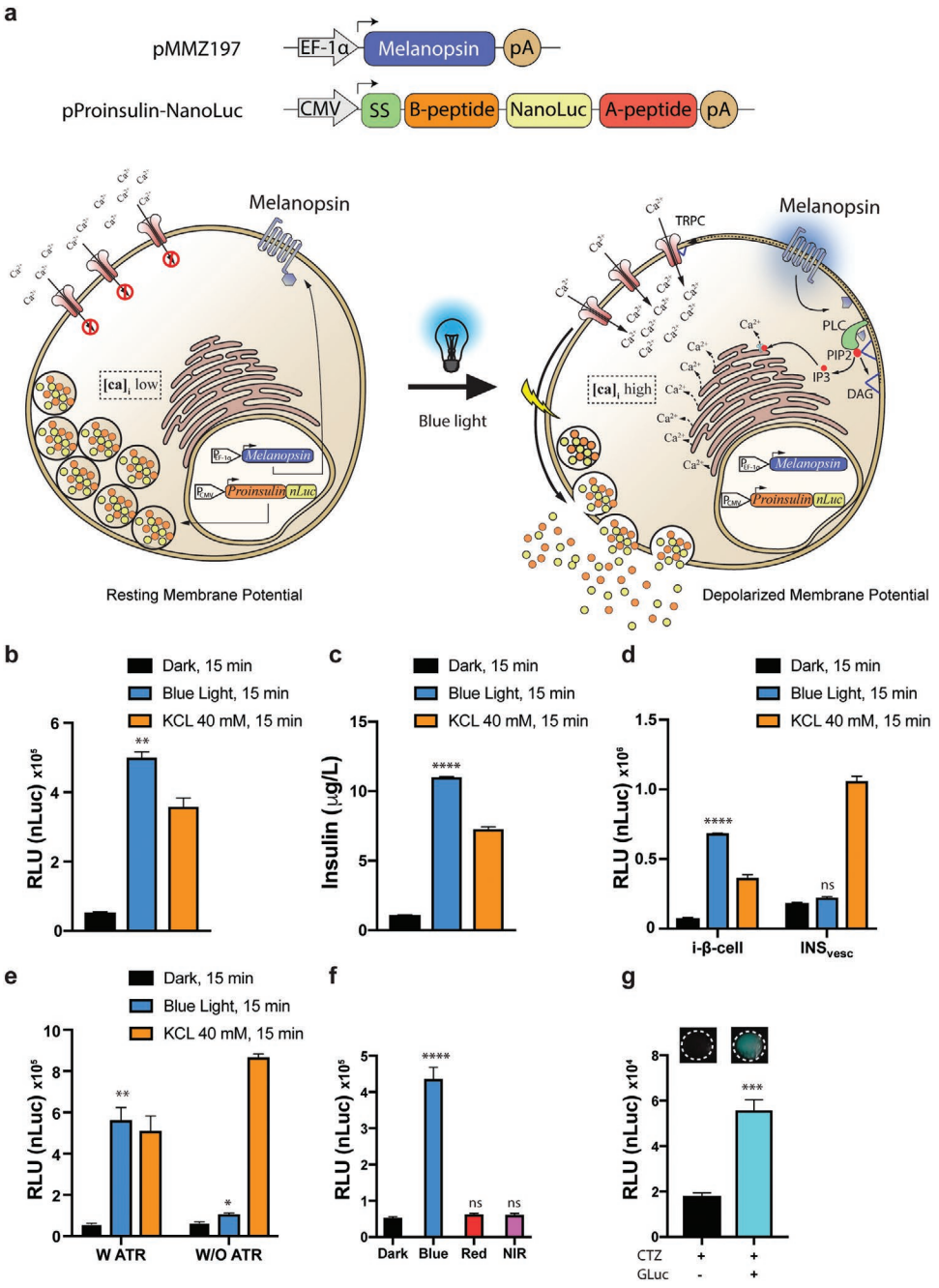

Figure 1. Design and validation of iβ-cells. a) Schematic representation of light-triggered rapid insulin-nLuc secretion in an iβ-cell. The iβ-cell line stably expresses melanopsin (pMMZ197; $P_{hEF\text{-}1\alpha}$-opn4-pA) as well as Proinsulin-nLuc (pProinsulin-nLuc; P_{CMV}-Proinsulin-nLuc-pA) and forms vesicular granules pre-loaded with insulin (red dots) and nLuc (yellow dots). Upon light stimulation, melanopsin triggers a calcium pathway that causes membrane depolarization and fusion of the vesicles with the plasma membrane, leading to release of insulin and nLuc. b) Cultured iβ-cells are stimulated with blue light (475 nm; 10 s ON and 5 s OFF and 300 μW cm^{-2}) followed by 40 mM KCl. Control cells are kept in the dark. Luminescence was measured in the supernatant every 15 min; $n = 3$. c) Insulin content in the supernatant of the same iβ-cells as used in (b) was measured by ELISA; $n = 3$. d) Melanopsin-dependent rapid secretion in iβ-cells. Cells expressing melanopsin (iβ-cells) or without melanopsin (INS_{vesc}) are exposed to light or kept in dark; $n = 3$. e) Ability of melanopsin to trigger insulin-nLuc secretion in the presence (W) or absence (W/O) of ATR in the culture medium. f) Activation of iβ-cells in response to light of different wavelengths. iβ-cells are exposed to blue (475 nm, 300 μW cm^{-2}), red (660 nm, 8 μW cm^{-2}), and NIR (740 nm, 1 mW cm^{-2}) light. $n = 6$. g) Bioluminescence-mediated rapid secretion in iβ-cells. Supernatant of cultured iβ-cells was replaced with media containing GLucM23 with or without CTZ substrate. nLuc levels are assessed in the supernatant of cultured cells 15 min after media exchange. Images of related wells are provided at the top of corresponding bar graphs; $n = 4$. Plots show the mean ± SEM. *P* values between illuminated and un-illuminated groups are determined using a two-tailed, paired (b–e) or unpaired (f–g) Student's *t*-test. ns: not significant, ***$P < 0.001$, ****$P < 0.0001$ (versus control).

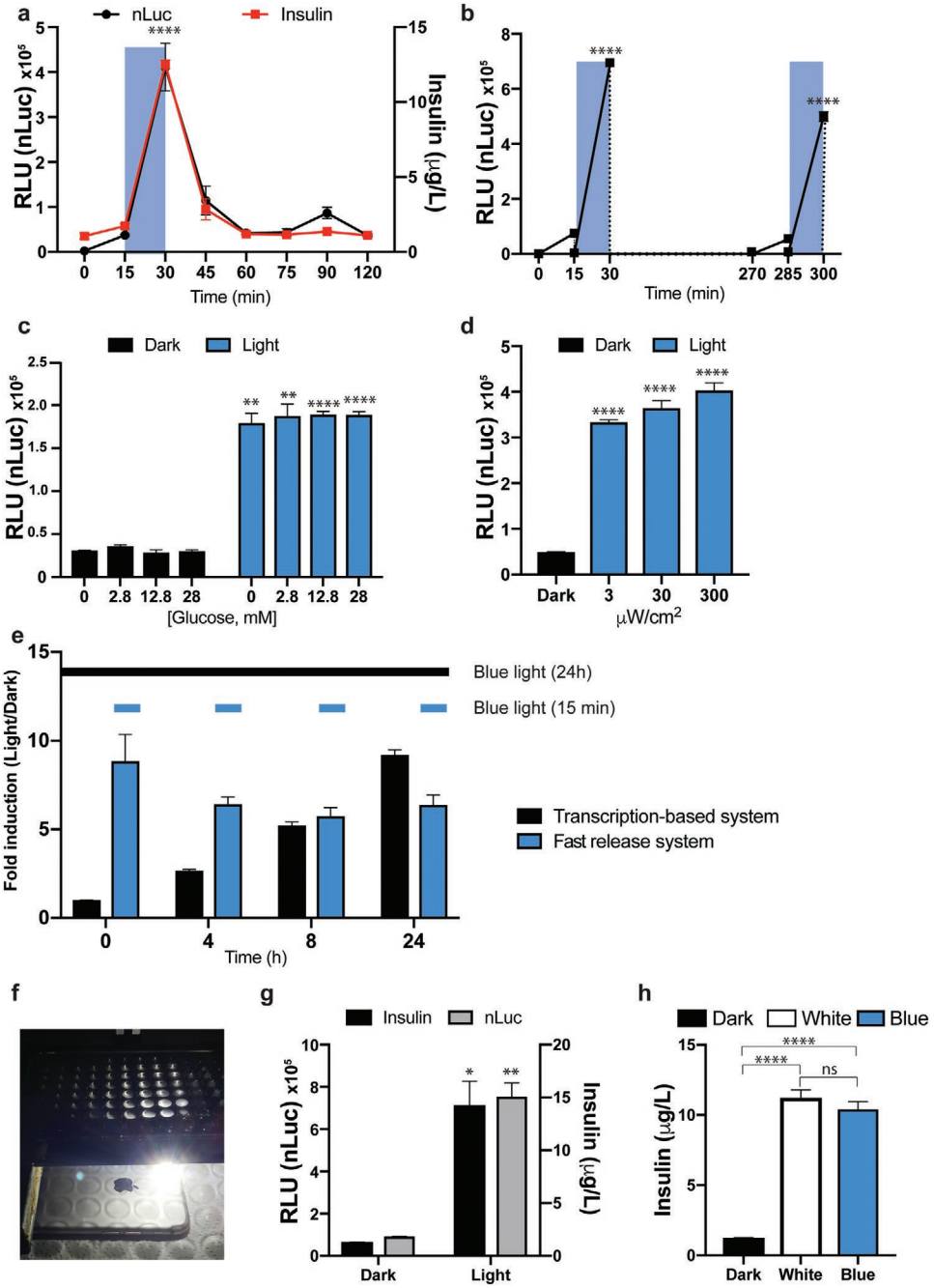

Figure 2. Characterization of iβ-cells. a) Release over time in iβ-cell lines. Cultured iβ-cells are stimulated with blue light (475 nm; 10 s ON and 5 s OFF and 300 µW cm^{-2}) for 15 min. nLuc levels are measured in supernatant of cultured cells every 15 min; $n = 6$. b) Reversibility assay. iβ-cells are stimulated for 15 min twice, with a 4-h time interval between the first and second light stimulations; 475 nm; 10 s ON and 5 s OFF and 300 µW cm^{-2}, $n = 3$. c) Exclusively light-induced secretion in iβ-cells. iβ-cells are incubated with various concentrations of glucose and exposed to light or kept in the dark; $n = 4$. d) Light-intensity-dependent iβ-cell activity. iβ-cells are illuminated with blue light of different intensities (0–300 µW cm^{-2}); $n = 3$. e) Comparative insulin-nLuc secretion kinetics. HEK293T cells are co-transfected with melanopsin (pHY42; P_{CMV}-opn4-pA) and a synthetic expression unit containing NFAT-responsive elements (pMMZ364; $P_{NFAT}P_{CMVmin}$-Igk-nLuc-2A-mINS-pA). These cells are illuminated with blue light (475 nm; 10 s ON and 5 s OFF and 300 µW cm^{-2}) for 24 h and insulin-nLuc secretion was assessed in the culture supernatant at the indicated time points. Likewise, iβ-cells are illuminated with blue light (475 nm; 10 s ON and 5 s OFF and 300 µW cm^{-2}) for 15 min at the indicated time points and the immediate insulin-nLuc release was monitored in the culture supernatant. Control cells are kept in dark; $n = 3$. f) Representative image of cultured iβ-cells that are exposed to the flashlight of a smartphone. g) The nLuc and insulin levels in the cell culture supernatant are assayed after 15 min of illumination by white light emitted from a smartphone. Control cells are kept in the dark. $n = 3$. h) Comparative levels of insulin secretion by iβ-cells upon illumination with blue or white light. Control cells are kept in the dark. $n = 4$. Plots show the mean ± SEM. P values between illuminated and un-illuminated groups are determined using a two-tailed, paired (a–c and g) or unpaired (d) Student's t-test as well as one-way ANOVA (h). ns: not significant, $^{**}P < 0.01$, $^{***}P < 0.001$, $^{****}P < 0.0001$ (versus control).

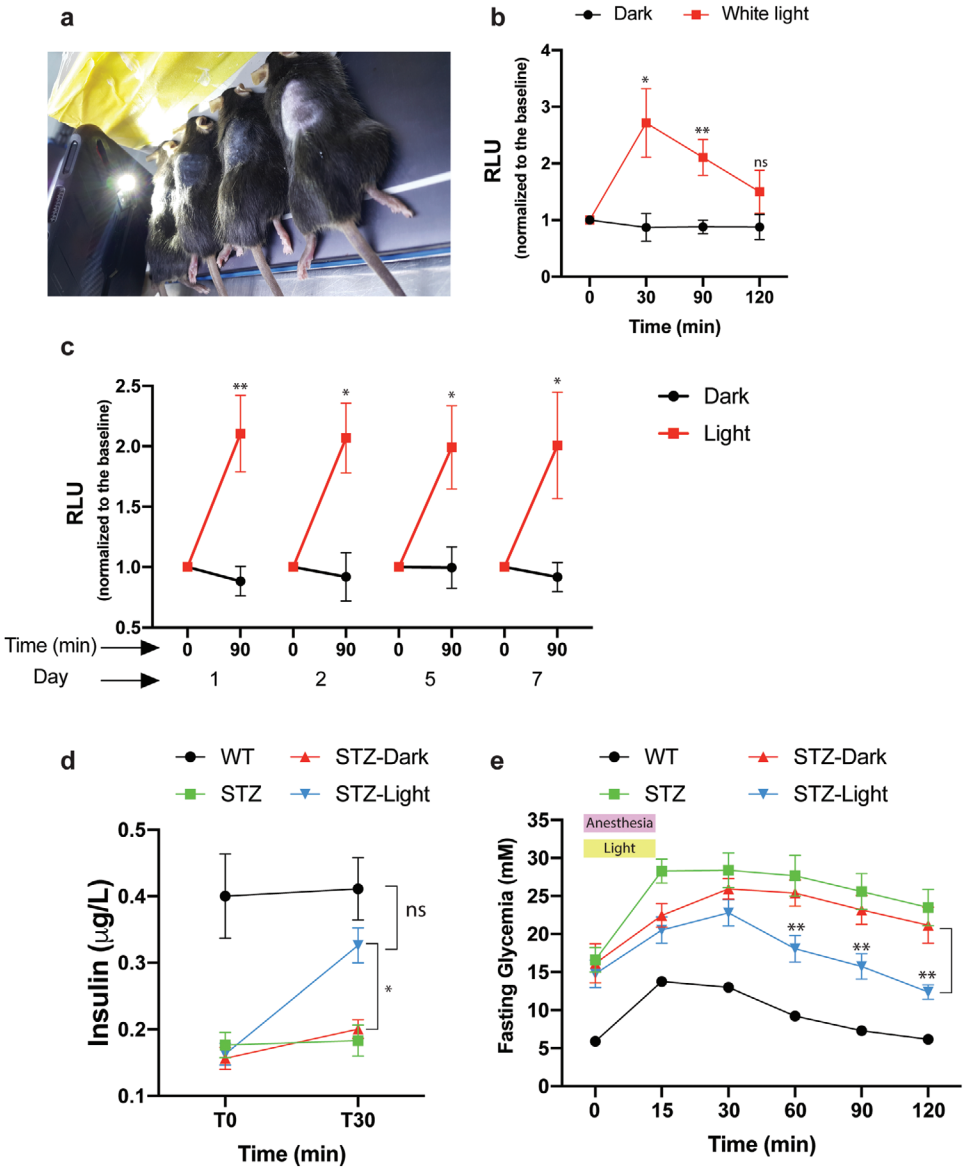

Figure 3. Smartphone-controlled rapid insulin secretion in type-1 diabetic mice. a) Representative image of C57BL/6JRj mouse subcutaneously implanted with microencapsulated iβ-cells and exposed to a smartphone's flashlight. b) In vivo time-resolved blood luciferase levels in wild-type C57BL/6JRj mice implanted with microencapsulated iβ-cells. Animals are illuminated for 15 min with white light (≈2–5 mW cm^{-2}) emitted from a smartphone. The nLuc levels are quantified from microliter-scale blood samples drawn every 30 min. Values are mean ± SEM, $n = 5$. P values between illuminated and un-illuminated groups of mice at indicated times are determined using a two-tailed, paired Student's t-test. c) In vivo reversibility and repeatability. Wild-type C57BL/6JRj are implanted with microencapsulated iβ-cells and irradiated for 15 min with a smartphone's flashlight (≈2–5 mW cm^{-2}) over a period of 7 days. Values are mean ± SEM, $n = 5$. P values between illuminated and un-illuminated groups of mice are determined using a two-tailed, paired Student's t-test. d) In vivo blood insulin levels in type-1 diabetic model mice. STZ-induced type-1 diabetic mice subcutaneously implanted with microencapsulated iβ-cells are fasted for 12 h and then exposed for 15 min to white light (≈2–5 mW cm^{-2}) from a smartphone flashlight. The insulin levels in the bloodstream are measured in all groups before and after illumination. Values are mean ± SEM, $n = 5$. P values between indicated groups of STZ-mice are determined using a one-way ANOVA. e) Intraperitoneal GTT (IPGTT) was performed by injection of 1.5 g kg^{-1} aqueous D-glucose and was conducted 6 h after implantation in overnight-starved animals. Animals in the illuminated group are anesthetized and irradiated with a smartphone's flashlight (≈2–5 mW cm^{-2}) for 15 min. Wild-type (WT) C57BL/6JRj mice (WT, $n = 5$) as well as STZ-induced type-1 diabetic mice (STZ, $n = 5$) without the cell implant are used as controls. Values are mean ± SEM. P values between illuminated ($n = 7$) and un-illuminated ($n = 7$) STZ groups are determined using a two-way ANOVA. ns: not significant, *$P < 0.05$, **$P < 0.01$ (versus control).

and Figure S8c, Supporting Information). To validate iβ-cells in a clinical proof-of-concept study, we used a smartphone to percutaneously program on-demand secretion of insulin for the treatment of experimental type-1 diabetes. For this purpose, streptozotocin (STZ)-induced type 1 diabetic mice[39] were subcutaneously implanted with microencapsulated iβ-cells. Exposure to white light illumination for 15 min led to an increased level of blood insulin level compared to mice kept in an

unstimulated state (Figure 3d). Also, a glucose tolerance test (GTT) revealed lower glucose levels in white-light-stimulated mice, in accordance with the restoration of postprandial glucose hemostasis in T1D mice mediated by our iβ-cells (Figure 3e).

3. Discussion and Conclusion

In this work, we applied a non-invasive light stimulus generated by flashlight of a smartphone to remotely program a rapid therapeutic response from engineered cells. The effectiveness of this technology was successfully validated in a mouse model of type-1 diabetes. Thus, the iβ-cells link optogenetic interventions to smartphones, a device owned by 81% of North American adults.[25] Today's smartphone sensor technology already enables continuous and remote monitoring services for individual health and fitness at an affordable price.[26,28] In addition, wearable electronic biosensors can provide real-time monitoring of disease-related biomarkers, such as blood glucose levels[40] or non-invasive monitoring in tears,[41] perspiration,[42] and interstitial fluids.[43] The continuously acquired data can be wirelessly transferred to a smartphone that runs self-learning AI-based algorithms for data analysis.[44] Such "digital therapeutics" can improve lifestyle[45] as well as disease self-management[46,47] in patients and is currently in U.S. Food and Drug Administration (FDA)-cleared or -approved clinical trials.[48,49] Nevertheless, both embedded smartphone sensors and wearable biosensor devices presently focus solely on data collection, and lack direct feedback-controlled intervention capabilities.

Closed-loop strategies in synthetic biology-inspired cell-based therapies rely on engineered artificial cells that induce expression of therapeutic genes in response to up-regulated disease-related biomarkers with negative feedback implemented to autonomously and self-sufficiently interface with the patient's metabolism.[15,50] However, such designer cells often work via transcription of therapeutic transgenes, which results in a marked delay in secretion of the therapeutic protein.[3–6] To overcome this issue, therapeutic designer cells based on open-loop strategies have been developed to rapidly release pre-formed therapeutics, such as insulin, in response to remote-control inducers, including electrostimulation[11] and light.[51,52] However, bioelectronic implants for electrogenetic control of glucose hemostasis require surgical implantation as well as a wireless power supply and control units, all of which are associated with real-world challenges and risks. Also, current optogenetic systems providing fast insulin release rely on bacterial components in their genetic circuits, which can trigger an adverse immune reaction.

In this study, we introduce smartphone flashlight control for rapid secretion of insulin from an engineered light-sensitive iβ-cell line. The combination of iβ-cells with digital technologies, such as wearable continuous glucose monitoring devices (biosensor platform) and smartphones (controller platform), could eventually enable full closed-loop control, a cell-based treatment strategy that can cure a variety of experimental metabolic disorders[3,4,53,54] or infectious diseases.[5,6] However, in order to translate this proof-of-concept smartphone-flashlight-controllable iβ-cell system into clinical reality, several limitations need to be considered. First, improved cell encapsulation strategies, including novel approaches and materials that ensure long-term cell survival, will be needed. Second, in order to establish a fully-humanized iβ-cell line, it will be necessary to replace the mouse insulin in the iβ-cell line with the human insulin sequence. Third, in this study, we did not implement a talk-back functionality that would enable the cells to directly communicate with the smartphone. Currently, wearable electronic devices can mediate the cell-to-smartphone connection, but alternatively, a biosensor platform could be incorporated in a future generation of the iβ-cell line by introducing genetic circuits with outputs (e.g., inducible bioluminescence upon hyperglycemia) that are directly detectable by smartphones.

In the future, a non-invasive iβ-cell-based system that produces insulin spontaneously and autonomously could play a role in disease self-management, in addition to purely electronic-based setups such as the FDA-approved artificial pancreas,[44] which requires invasive continuous blood-glucose monitoring together with real-time injection of exogenously provided insulin.

4. Experimental Section

Molecular Cloning and DNA Constructs: Comprehensive design and construction details of the expression vectors were provided in Tables S1 and S2, Supporting Information.

Cell Culture and Transient Transfection: Human embryonic kidney cells (ATCC: CRL3216, HEK-293T) were cultured in Dulbecco's modified Eagle's medium (DMEM; Life Technologies, Carlsbad, CA, USA) supplemented with 10% (v/v) fetal bovine serum (FBS; Sigma-Aldrich Munich, Germany) and 1% (v/v) penicillin/streptomycin solution (P/S: 100 U mL^{-1} penicillin and 100 µg mL^{-1} streptomycin, Sigma-Aldrich, Munich, Germany). 1.1E7 cells (cat. no. 10070101-1VL, Sigma-Aldrich, Saint Louis, MO, USA) were cultivated in Roswell Park Memorial Institute 1640 medium (RPMI; cat. no. 72400-021, Thermo Fischer Scientific) supplemented with 10% FBS and 1% (v/v) P/S. Cell culture media were supplemented with 5 μ_M ATR (cat. no. R2500, Sigma-Aldrich) at 15 min before the start of the illumination experiment. All cells were cultured in a humidified atmosphere containing 5% CO2 at 37 °C. Cell viability and number were assessed with an electric field multi-channel cell-counting device (CASY Cell Counter and Analyzer Model TT; Roche Diagnostics GmbH, Basel, Switzerland). For transfection, 6.2×104 cells were seeded per plate of a 24-cell culture dish, and incubated for 24 h. Then, they were transfected with Lipofectamine 3000 according to the manufacturer's instructions. 3D-cell culture was performed in AggreWellTM400 plates (Stem Cell Technology, Canada) pre-treated with Anti-Adherence Rinsing Solution (cat. No. 0 7010, Stem Cell Technology, Canada). For adherent (2D) culture, cells were plated in a 96-well black plate with a transparent bottom (cat. No. 655 090, Greiner bio-one, Germany) and pre-treated with poly-L-lysine (cat. No. A-005-C, Merck, Germany).

Illumination Experiment: A 96-LED array platform with multiple tunable parameters was constructed (including light intensities and irradiation pattern) for illumination of individual wells in 96-well microwell plates.[55] An Arduino control script for the custom-designed LED-microwell plate was provided in Note S1, Supporting Information. Cells were irradiated with a blue LED (475 nm, B56L5111P, Roithner LaserTechnik, Austria), white LED (W54L5111P, Roithner LaserTechnik, Austria), or a smartphone flashlight (Samsung note 4 or iPhone 7). For the in vivo experiment, we used either the smartphone flashlight (Samsung note 4 and iPhone 7) or the programmed 96-LED microwell platform. In the bioluminescence-mediated illumination experiment, HEK293 cells were transfected with pMMZ112 (PCMV-hGluc-pA) and the medium containing secreted GLuc was harvested after 2 days. This medium containing coelenterazine (CTZ) (cat. no. 303-5; Nanolight Technologies, USA) was used for bioluminescence-based light production. Intensities of blue and white light were measured using a photometer (Ophir Photonics, Israel) at 475 nm.

Generation of Stable Cell Lines: A 1.1E7-derived cell clone deficient in glucose-sensitive insulin secretion was transduced with Proinsulin-NanoLuc-derived lentiviral particles and selected in culture medium containing 5 μg mL^{-1} blasticidin to create polyclonal INSvesc cells.[11] Next, a monoclonal cell population, INSvesc-A12-A15, was picked based on the best performance for depolarization-triggered nLuc secretion. This cell line was co-transfected with the SB100X expression vector pCMV-T7-SB100 (PhCMV-SB100X-pA) and the SB100X-specific transposon pMMZ197 (ITR-PhEF1α-melanopsin-pA-PRPBSA-ypet-P2A-PuroR-pA-ITR) to generate a polyclonal population of iβ-cells that stably expressed melanopsin as well as Proinsulin-NanoLuc cassettes. After selection for two weeks in medium containing 5 μg mL^{-1} blasticidin and 1 μg mL^{-1} puromycin, the monoclonal iβ-cells were sorted by means of FACS (Becton Dickinson LSRII Fortessa flow cytometer) into three different subpopulations according to their Ypet fluorescence intensities (high, middle, low), and each individual sorted cell was grown in a well of a 96-well plate. Monoclonal cell populations were screened for blue-light-responsive nLuc secretion. iβ-cell_H7 was selected as the best performer and was used for follow-up experiments.

Microscopy: Cells for microscopic analysis were plated in black 96-well plates, F-bottom (Greiner bio one, lot # E18053JY) treated with poly-L-lysine (cat. No. P4707, Sigma-Aldrich). Analysis of cells was performed 48 h after transfection. Cells were fixed with 4% formaldehyde in PBS and stained with DAPI. Imaging was performed on a Leica SP8 laser-scanning confocal microscope. DAPI and eGFP were excited with the 405 and 514 nm laser lines and emission was acquired from 430 to 450 nm (DAPI; 405/430-450) and 525–545 nm (GFP; 514/525-545), respectively.

Calcium imaging was done by staining iβ-cell_H7 with Rhod-2, AM dye (cat. No. R1244, Invitrogen) and recording changes in fluorescence on a Nikon Ti2 microscope equipped with a motorized stage, temperature-controlled environment, Plan Apo VC 20x lenses, a Hamamatsu Orca Flash 4.0 V2 camera and a Spectra Lumencore light source. Rhod-2, AM dye was resuspended in DMSO to a final concentration of 5 mM and cells were incubated for 20 min in culture medium containing 5 μ_M Rhod-2, AM. Following staining, medium was exchanged and cells were incubated for another 20 min in standard cell culture medium supplemented with 5 μ_M ATR prior to measurement. Images were taken from the center of each well. During imaging, we first recorded a reference image at 50 msec exposure time followed by the "Dark" image 100 msec later. Cells were then imaged for 5 s at 1 s intervals with simultaneous stimulation of melanopsin (488 and 560 nm excitation, 580 nm emission). Fluorescence intensities were measured for each image using Fiji software. Calcium responses were calculated as changes in fluorescence intensity upon stimulation compared to fluorescence derived from the first frame (dF/F0).

Analytical Assays: The levels of mouse insulin (mINS) in culture supernatants and mouse serum were quantified with a Rat/Mouse Insulin ELISA kit (Mercodia; cat. no.10-1232-01) and Ultrasensitive Mouse Insulin ELISA kit (Mercodia; cat. no. 10-1249-01), respectively. NanoLuc levels in cell culture supernatants were quantified using the Nano-Glo Luciferase Assay System (N1110, Promega). For the quantification of human placental-SEAP, cell culture supernatant was heat-inactivated for 30 min at 65 °C. Then, 10 μL supernatant was diluted with 90 μL dH_2O and mixed with 80 μL 2 × SEAP buffer (20 mM homoarginine, 1 mM MgCl2, 21% (v/v) diethanolamine, pH 9.8) and 20 μL of substrate solution containing 20 mM pNPP (Acros Organics BVBA) in 2× SEAP buffer. Measurement was performed at 405 nm using a Tecan microplate reader (TECAN AG, Maennedorf, Switzerland). The cytotoxic effect of light on illuminated cells was monitored by means of MTT assay (Sigma-Aldrich, Munich, Germany; cat. no. M5655). In brief, after 15 min illumination of cells with blue light, the medium was replaced with culture medium containing 20 mM resazurin and incubation was continued for 2–4 h. The absorbance of resazurin was quantified on a Tecan microplate reader with excitation at 570 nm and emission at 590 nm. For the GTT, mice were challenged by intraperitoneal injection of glucose (1.5 g kg^{-1} body weight in H2O) and the glycemic profile was obtained by measurement of blood glucose levels with a glucometer (Contour Next; Bayer HealthCare, Leverkusen, Germany) every 15 or 30 min for 120 min.

Cell Encapsulation: iβ-cells were encapsulated with an Inotech Encapsulator Research Unit IE-50R (EncapBioSystems Inc., Greifensee, Switzerland). Coherent alginate-poly-(L-lysine) beads (400 μm diameter, 2000 cells per capsule) were generated with the following parameters: 200-μm nozzle with a vibration frequency of 1000 Hz; 25-mL syringe operated at a flow rate of 410 units; 1.2 kV bead dispersion voltage.

Animal Study: All experiments involving animals were performed in accordance with the Swiss animal welfare legislation and approved by the veterinary office of the Canton Basel-Stadt (approval no. 2879/31 996).

Experimental Animals: Male wild-type C57BL/6JRj mice, aged 8–9 weeks were obtained from Janvier Labs (Saint-Berthevin, France) and acclimatized for at least 1 week. Type-1 diabetic model mice were generated by intraperitoneal injection of STZ for 5 days at a dose of 60 mg kg^{-1} per day in male C57BL/6J mice weighing at least 25 g. One week after STZ injection, fasting blood glucose as well as fasting insulin levels were monitored in STZ-treated mice and compared with those of wild-type mice. STZ-treated mice with a level of blood glucose higher than 15 mM and fasting insulin level lower than that of wild-type mice were considered as diabetic mice. Animals were housed with an inverse 12 h day-night cycle in a temperature (21 ± 2 °C) and humidity (55 ± 10%)-controlled room with ad libitum access to standard diet and drinking water. Animals were randomly assigned to experimental groups.

Implantation Experiments: Implantation was performed by subcutaneous injection of 1 mL glucose-free DMEM containing alginate-poly(L-lysine)-alginate-microencapsulated 3 × 106 iβ-cells in the shaved back on one side of the mice. At 4 h after implantation, either a custom-built LED platform or smartphone was applied to illuminate the injection site. Plasma was collected by centrifugation (10 min, 5 000 g) of clotted blood (20 min at 37 °C and then 20 min at 4 °C).

Statistical Analysis: A two-tailed, paired or unpaired, Student's *t*-test, one-way ANOVA, or two-way ANOVA was applied as appropriate to determine the statistical significance of differences among groups, using GraphPad Prism. The test used and the significance of differences were shown in the figures and their legends.

Data Availability: Requests for materials should be made to the corresponding author. All plasmids generated in this study are available upon request. All data are available upon reasonable request.

Supporting Information

Supporting Information is available from the Wiley Online Library or from the author.

Acknowledgements

Work in the laboratory of M.F. is financially supported in part through a European Research Council advanced grant (ElectroGene, no. 785800) and in part by the National Center of Competence in Research (NCCR) for Molecular Systems Engineering as well as the EC Horizon 2020 Framework Programme ENLIGHT (no. 964497). The authors would like to thank Ute Hochgeschwender for providing LMO4 plasmid and Mingqi Xie for generous advice.

Conflict of Interest

The authors declare no conflict of interest.

Author Contributions

M.M. and M.F. designed the project, M.M. and T.S. conducted in vitro experiments, G.C. designed the animal experiments, S.X., M.D.H and M.M. performed animal experiments, M.M. and M.F. analysed the data and wrote the manuscript.

Data Availability Statement

The data that support the findings of this study are available from the corresponding author upon reasonable request.

Keywords

cell-based therapies, optogenetics, smartphone, synthetic biology, type-1 diabetes

Received: April 1, 2021
Revised: April 26, 2021
Published online:

[1] T. Kitada, B. DiAndreth, B. Teague, R. Weiss, *Science* **2018**, *359*, eaad1067.
[2] L. Scheller, M. Fussenegger, *Curr. Opin. Biotechnol.* **2019**, *58*, 108.
[3] M. Xie, H. Ye, H. Wang, G. Charpin-El Hamri, C. Lormeau, P. Saxena, J. Stelling, M. Fussenegger, *Science* **2016**, *354*, 1296.
[4] K. Rössger, G. Charpin-El-Hamri, M. Fussenegger, *Nat. Commun.* **2013**, *4*, 2825.
[5] F. Sedlmayer, T. Jaeger, U. Jenal, M. Fussenegger, *Nano Lett.* **2017**, *17*, 5043.
[6] Y. Liu, P. Bai, A. K. Woischnig, G. Charpin-El Hamri, H. Ye, M. Folcher, M. Xie, N. Khanna, M. Fussenegger, *Cell* **2018**, *174*, 259.
[7] H. Ye, M. D. El Baba, R. W. Peng, M. Fussenegger, *Science* **2011**, *332*, 1565.
[8] D. Bojar, L. Scheller, G. C. El Hamri, M. Xie, M. Fussenegger, *Nat. Commun.* **2018**, *9*, 2318.
[9] J. Yin, L. Yang, L. Mou, K. Dong, J. Jiang, S. Xue, Y. Xu, X. Wang, Y. Lu, H. Ye, *Sci. Transl. Med.* **2019**, *11*, eaav8826.
[10] S. Xue, J. Yin, J. Shao, Y. Yu, L. Yang, Y. Wang, M. Xie, M. Fussenegger, H. Ye, *Mol. Ther.* **2017**, *25*, 443.
[11] K. Krawczyk, S. Xue, P. Buchmann, G. Charpin-El-Hamri, P. Saxena, M. D. Hussherr, J. Shao, H. Ye, M. Xie, M. Fussenegger, *Science* **2020**, *368*, 993.
[12] S. A. Stanley, J. E. Gagner, S. Damanpour, M. Yoshida, J. S. Dordick, J. M. Friedman, *Science* **2012**, *336*, 604.
[13] Y. Pan, S. Yoon, J. Sun, Z. Huang, C. Lee, M. Allen, Y. Wu, Y. J. Chang, M. Sadelain, K. K. Shung, S. Chien, Y. Wang, *Proc. Natl. Acad. Sci. U. S. A.* **2018**, *115*, 992.
[14] I. C. Miller, M. Gamboa Castro, J. Maenza, J. P. Weis, G. A. Kwong, *ACS Synth. Biol.* **2018**, *7*, 1167.
[15] M. Xie, M. Fussenegger, *Nat. Rev. Mol. Cell Biol.* **2018**, *19*, 507.
[16] K. S. Polonsky, B. D. Given, E. Van Cauter, *J. Clin. Invest.* **1988**, *81*, 442.
[17] A. Katsarou, S. Gudbjörnsdottir, A. Rawshani, D. Dabelea, E. Bonifacio, B. J. Anderson, L. M. Jacobsen, D. A. Schatz, A. Lernmark, *Nat. Rev. Dis. Prim.* **2017**, *3*, 1.
[18] M. Ezzati, S. Vander Hoorn, A. D. Lopez, G. Danaei, A. Rodgers, C. D. Mathers, C. J. L. Murray, *Global Burden of Disease and Risk Factors*, Oxford University Press, New York, **2006**, Ch. 4.
[19] K. E. Kreider, A. A. Gabrielski, F. B. Hammonds, *Nurs. Clin. North Am.* **2018**, *53*, 303.
[20] G. Umpierrez, M. Korytkowski, *Nat. Rev. Endocrinol.* **2016**, *12*, 222.
[21] A. L. McCall, L. S. Farhy, *Minerva Endocrinol* **2013**, *38*, 145.
[22] K. S. Polonsky, *N. Engl. J. Med.* **2012**, *367*, 1332.
[23] L. A. DiMeglio, C. Evans-Molina, R. A. Oram, *Lancet* **2018**, *391*, 2449.
[24] V. M. Rivera, X. Wang, S. Wardwell, N. L. Courage, A. Volchuk, T. Keenan, D. A. Holt, M. Gilman, L. Orci, F. Cerasoli, J. E. Rothman, T. Clackson, *Science* **2000**, *287*, 826.
[25] I. Sim, *N. Engl. J. Med.* **2019**, *381*, 956.
[26] S. R. Steinhubl, E. D. Muse, E. J. Topol, *Sci. Transl. Med.* **2015**, *7*, 283rv3.
[27] N. Koenig, A. Seeck, J. Eckstein, A. Mainka, T. Huebner, A. Voss, S. Weber, *Telemed. e-Health* **2016**, *22*, 631.
[28] S. Majumder, M. J. Deen, *Sensors* **2019**, *19*, 2164.
[29] J. Kim, A. S. Campbell, B. E. F. de Ávila, J. Wang, *Nat. Biotechnol.* **2019**, *37*, 389.
[30] K. Kalantar-Zadeh, N. Ha, J. Z. Ou, K. J. Berean, *ACS Sens.* **2017**, *2*, 468.
[31] J. X. J. Zhang, K. Hoshino, in *Mol. Sensors Nanodevices*, Elsevier, **2014**, pp. 415–465.
[32] D. V. Dimitrov, *Healthc. Inform. Res.* **2016**, *22*, 156.
[33] J. Goecks, V. Jalili, L. M. Heiser, J. W. Gray, *Cell* **2020**, *181*, 92.
[34] J. Lang, *Eur. J. Biochem.* **1999**, *259*, 3.
[35] J. A. Frank, J. Broichhagen, D. A. Yushchenko, D. Trauner, C. Schultz, D. J. Hodson, *Nat. Rev. Endocrinol.* **2018**, *14*, 721.
[36] R. D. Airan, K. R. Thompson, L. E. Fenno, H. Bernstein, K. Deisseroth, *Nature* **2009**, *458*, 1025.
[37] J. T. McCluskey, M. Hamid, H. Guo-Parke, N. H. McClenaghan, R. Gomis, P. R. Flatt, *J. Biol. Chem.* **2011**, *286*, 21982.
[38] S. M. Burns, A. Vetere, D. Walpita, V. Dančík, C. Khodier, J. Perez, P. A. Clemons, B. K. Wagner, D. Altshuler, *Cell Metab.* **2015**, *21*, 126.
[39] M. Kleinert, C. Clemmensen, S. M. Hofmann, M. C. Moore, S. Renner, S. C. Woods, P. Huypens, J. Beckers, M. H. De Angelis, A. Schürmann, M. Bakhti, M. Klingenspor, M. Heiman, A. D. Cherrington, M. Ristow, H. Lickert, E. Wolf, P. J. Havel, T. D. Müller, M. H. Tschöp, *Nat. Rev. Endocrinol.* **2018**, *14*, 140.
[40] J. B. Welsh, P. Gao, M. Derdzinski, S. Puhr, T. K. Johnson, T. C. Walker, C. Graham, *Diabetes Technol. Ther.* **2019**, *21*, 128.
[41] V. L. Alexeev, S. Das, D. N. Finegold, S. A. Asher, *Clin. Chem.* **2004**, *50*, 2353.
[42] W. Gao, S. Emaminejad, H. Y. Y. Nyein, S. Challa, K. Chen, A. Peck, H. M. Fahad, H. Ota, H. Shiraki, D. Kiriya, D. H. Lien, G. A. Brooks, R. W. Davis, A. Javey, *Nature* **2016**, *529*, 509.
[43] A. J. Bandodkar, W. Jia, C. Yardimci, X. Wang, J. Ramirez, J. Wang, *Anal. Chem.* **2015**, *87*, 394.
[44] S. A. Brown, B. P. Kovatchev, D. Raghinaru, J. W. Lum, B. A. Buckingham, Y. C. Kudva, L. M. Laffel, C. J. Levy, J. E. Pinsker, R. P. Wadwa, E. Dassau, F. J. Doyle, S. M. Anderson, M. M. Church, V. Dadlani, L. Ekhlaspour, G. P. Forlenza, E. Isganaitis, D. W. Lam, C. Kollman, R. W. Beck, *N. Engl. J. Med.* **2019**, *381*, 1707.
[45] S. E. Bonn, M. Löf, C. G. Östenson, Y. T. Lagerros, *BMC Public Health* **2019**, *19*, 273.
[46] E. Arsand, M. Muzny, M. Bradway, J. Muzik, G. Hartvigsen, *J. Diabetes Sci. Technol.* **2015**, *9*, 556.
[47] G. Fagherazzi, P. Ravaud, *Diabetes Metab.* **2019**, *45*, 322.
[48] "FDA clears mobile medical app to help those with opioid use disorder stay in recovery programs | FDA,", https://www.fda.gov/news-events/press-announcements/fda-clears-mobile-medical-app-help-those-opioid-use-disorder-stay-recovery-programs.
[49] "Teva Pharmaceutical Industries Ltd. – Teva Announces FDA Approval of AirDuo® Digihaler™ (fluticasone propionate 113 mcg and salmeterol 14 mcg) Inhalation Powder,", https://ir.tevapharm.com/news-and-events/press-releases/press-release-details/2019/Teva-Announces-FDA-Approval-of-AirDuosupregsup-Digihalertrade-fluticasone-propionate-113-mcg-and-salmeterol-14-mcg-Inhalation-Powder/default.aspx.
[50] M. Xie, M. Fussenegger, *Biotechnol. J.* **2015**, *10*, 10051018.
[51] F. Zhang, E. S. Tzanakakis, *ACS Synth. Biol.* **2019**, *8*, 2248.
[52] T. Kushibiki, S. Okawa, T. Hirasawa, M. Ishihara, *Gene Ther.* **2015**, *22*, 553.
[53] H. Ye, M. Xie, S. Xue, G. C.-E. El Hamri, J. Yin, H. Zulewski, M. Fussenegger, *Nat. Biomed. Eng.* **2017**, *1*, 0005.
[54] C. Kemmer, M. Gitzinger, M. Daoud-El Baba, V. Djonov, J. Stelling, M. Fussenegger, *Nat. Biotechnol.* **2010**, *28*, 355.
[55] M. Mansouri, S. Lichtenstein, T. Strittmatter, P. Buchmann, M. Fussenegger, in *Methods in Molecular Biology*, Humana Press Inc., Totowa, NJ **2020**, pp. 189–199.